

LA-UR-22-20647

Approved for public release; distribution is unlimited.

Title: Improving Effective Mass Estimations in Pu-Metal Annuli

Author(s): Bourque, Cade Michael
Thompson, Cole Joseph
O'Neil, Brian Erick

Intended for: Report

Issued: 2022-01-25



Los Alamos National Laboratory, an affirmative action/equal opportunity employer, is operated by Triad National Security, LLC for the National Nuclear Security Administration of U.S. Department of Energy under contract 89233218CNA000001. By approving this article, the publisher recognizes that the U.S. Government retains nonexclusive, royalty-free license to publish or reproduce the published form of this contribution, or to allow others to do so, for U.S. Government purposes. Los Alamos National Laboratory requests that the publisher identify this article as work performed under the auspices of the U.S. Department of Energy. Los Alamos National Laboratory strongly supports academic freedom and a researcher's right to publish; as an institution, however, the Laboratory does not endorse the viewpoint of a publication or guarantee its technical correctness.

Improving Effective Mass Estimations in Pu-Metal Annuli

Cade M. Bourque, Cole J. Thompson, Brian E. O’Neil

Los Alamos National Laboratory, PT-3, P.O. Box 1663, Los Alamos, New Mexico 87544,
[*cbourque@lanl.gov*](mailto:cbourque@lanl.gov)

Abstract

Determining the effective mass of ^{240}Pu in a plutonium metal item can be achieved through a number of destructive and non-destructive assay techniques. However, these techniques have one or more shortcomings. These include the need for large quantities of plutonium, long measurement time, or lack of sufficient accuracy. While efforts have been made to mitigate these issues by estimating ^{240}Pu quantities through neutron coincidence counting techniques, these estimates are subject to systematic bias, and their estimates are not well characterized when other factors of the annulus’ physical form and composition are accounted for. In this work, we expand upon these non-destructive assay techniques via the implementation of random forest machine learning models, which produce correction functions that augment and improve the effective mass estimates derived from classical leakage multiplication, singles, doubles, and triples multiplicity counting equations.

Keywords

Neutron Coincidence Counting, Neutron Multiplicity Counting, Non-Destructive Assaying, Machine Learning

Highlights

- Effective mass estimates using the point model and multiplicity counting models for a dataset of 46,461 annuli are generally good, but produce significantly inaccurate estimates when working with sufficiently high or low mass samples
- Using the multiplicity counting method yields the most accurate effective mass estimate on average, but exhibits strongest bias (i.e., at higher doubles rates, estimates tend to under-predict the actual effective mass); conversely, the doubles point method produces the least accurate m_{eff} estimate on average, but is the least biased estimator.
- Random forest regression models trained on a the original 46,461 annuli (the “training set”) were employed to generate correction functions, $C_f(D)$, which predict the degree to which the point and multiplicity counting models overestimate/underestimate an annulus’ effective mass and produce a correction factor from the doubles rate to scale the initial estimate to offset this inaccuracy. When applied to test set of 1,000 randomly generated annuli, these correction functions improved the precision with which effective mass estimates were made, reducing the variance in these estimates
- An exponential correction factor, derived from annuli thickness and outer radius data, can greatly improve the precision of effective mass estimates by adjusting multiplicity counting model predictions. When applied to a set of 1,000 test annuli, the corrected multiplicity counting method estimates display an average estimated-known effective mass ratio value of $\overline{r_{e-k,c}} = 1.005$ and a standard deviation of $\sigma = 0.0065$.

1. Introduction

As part Los Alamos National Laboratory’s (LANL) plutonium operations, plutonium metal is purified via an electrorefining process. The end product of this refinement is highly pure, annular Pu castings, which go on to be used in various other activities. Obtaining precise and accurate knowledge of these samples’ masses, namely its ^{240}Pu contents, at this stage is highly important, as lacking this knowledge would undermine the success and efficacy of LANL’s nuclear material accountancy systems. While traditional and currently-employed assaying technique provide sufficient accuracy in Pu mass quantification, these approaches have their drawbacks; they either require some of the sample be destroyed to facilitate examination, they require large time investments, or they fail to precisely characterize abnormally large or small mass samples ($m < 210\text{ g}$ and $m > 3,864\text{ g}$, respectively). While progress has been made to mitigate these issues through the works of Hauck and Henzl (2014) [1] and Krick, Geist, and Mayo (2005) [2], in which neutron coincidence counting techniques are coupled with neutron weighted point models to derive effective mass estimates, the validity of this technique has only been demonstrated for Pu samples in cylindrical form-factors, and cannot be readily applied to this situation.

In this paper, we detail the development and application of a machine learning model which, when fed specific information regarding a Pu annulus’ composition and/or physical form, produces “correction functions”. When assessed at the annulus’ detected doubles emission (the function’s independent variable), this yields a correction factor, which is used to improve the accuracy and precision of the initial estimate of the annulus’ ^{240}Pu effective mass, m_{eff} .

2. Methodology

2.1. M_L Estimation Using Neutron Multiplicity Counting Method

The training data for this work comes from MCNP6.2 simulations of 46,461 distinct annuli, whose total masses fall between 100 g and 4,000 g, and who embody various combinations of height, outer radii, enrichment, ring thicknesses (defined as the difference between the outer and inner radii), and location (a surrogate parameter of an detection efficiency term within a proposed ^3He neutron detector [3]). Table 1, below, outlines the bounds and/or discrete values the various physical parameters of the annuli may assume.

Parameter	Values	Units
Height, H	1, 2, 3, ... , 11, 12	cm
Outer Radius, R	$0.4953 \leq OR \leq 5.08$	cm
Ring Thickness, T	0.254, 0.381, 0.508, 1.27, 2.54	cm
^{240}Pu Enrichment, E	0.5, 1.0, 2.0, 4.0, 6.0, 8.0	at%
Location, L	x1, x2, x3, ... , x8, xcenter	-
Density, ρ	19.86	$\frac{g}{cm^3}$

Table 1: Parameters for modeled annuli. See Figure A.1 for illustration of “Location” arrangement.

The detector environment in which the annuli are modeled is comprised of a neutron multiplicity detector attached to the exterior of a glove box. The annulus, placed inside of the detector, atop a CLYC scintillation crystal, is surrounded on three sides by a total 66 ^3He neutron detectors (Figure 1). Each MCNP test is programmed to execute 3.1×10^6 spontaneous fissions events, uniformly distributed throughout the annulus, and logs the total number of neutrons captured by each of the three ^3He detector tube sets via F8 capture tallies.

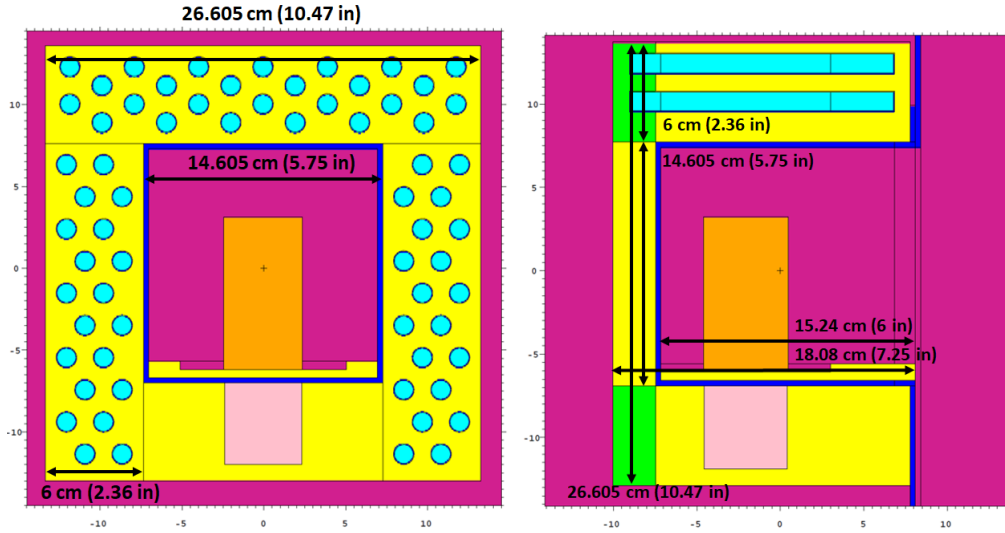


Figure 1: Diagram of annulus in proposed multiplicity counter. Front view (left) and side view (right) [3].

Upon the completion of each MCNP run, the values for the following system variables are extracted from the MCNP output file and recorded for later use:

- Detector efficiency: ε
- Double and triple gate fractions: f_d & f_t
- Single, doubles, and triples neutron capture rate: S , D , & T
- 2nd and 3rd reduced moments of the spontaneous fission neutron distribution: v_{s2} & v_{s3}
- 1st, 2nd, and 3rd reduced moments of the induced fission neutron distribution: v_{i1} , v_{i2} , & v_{i3}

These variables are then processed using the multiplicity counting method (MCM) [5], in which the above-listed system variables are inserted in Equations 1, 2, and 3. When evaluated, these provide coefficient values which can be substituted into Equation 4. Solving this cubic equation for its non-complex, real root(s) returns the expected net leakage multiplier for the annulus, M_L [5][6][7].

$$a + bM_L + cM_L^2 + M_L^3 = 0 \quad \text{Eq. 1}$$

$$a = \frac{-6Tv_{s2}(v_{i1} - 1)}{\varepsilon^2 f_t S(v_{s2}v_{i3} - v_{s3}v_{i2})} \quad \text{Eq. 2}$$

$$b = \frac{2D[v_{s3}(v_{i1} - 1) - 3v_{s2}v_{i2}]}{\varepsilon f_d S(v_{s2}v_{i3} - v_{s3}v_{i2})} \quad \text{Eq. 3}$$

$$c = \frac{6Dv_{s2}v_{i2}}{\varepsilon f_d S(v_{s2}v_{i3} - v_{s3}v_{i2})} - 1 \quad \text{Eq. 4}$$

2.2. Effective Mass Estimation

The effective mass of an annulus is defined as the mass of ^{240}Pu that would yield an equivalent neutron doubles rate to that produced by the combined spontaneous fission decays of ^{238}Pu , ^{240}Pu , and ^{242}Pu . This quantity can be determined using Eq. 5, in which m_{238} , m_{240} , and m_{242} correspond to the actual mass of ^{238}Pu , ^{240}Pu , and ^{242}Pu within the annulus, respectively. In this study, this equation is used to determine a known effective mass, $m_{eff,K}$. This is possible given that we have exact knowledge of the annuli's composition, as we defined such values in the creation of our MCNP models.

$$m_{eff,K} = 2.52m_{238} + m_{240} + 1.68m_{242} \quad \text{Eq. 5}$$

In practice, however, exact knowledge of an annuli's precise mass cannot be determined without first assaying the sample. Thus, Eq. 5 cannot be used if perfect knowledge of the annuli's composition is not assumed. In this case, other methods must be employed to estimate the value of m_{eff} . In this study, three different approaches are employed: the singles point model (SPM) seen in Eq. 6, the doubles point model (DPM) seen in Eq. 7, and the MCM in Eq. 8.

$$m_{eff,S} = \frac{S}{F\varepsilon M_L v_{s1}(1 + \alpha)} \quad \text{Eq. 6}$$

$$m_{eff,D} = \frac{2D}{F\varepsilon^2 f_d M_L^2 \left[v_{s2} + \frac{M_L - 1}{v_{i1} - 1} v_{s1} v_{i2} (1 + \alpha) \right]} \quad \text{Eq. 2.7}$$

$$m_{eff,M} = \frac{\left[\frac{2D}{\varepsilon f_d} - \frac{M_L(M_L - 1)v_{i2}S}{v_{i1} - 1} \right]}{473\varepsilon M_L^2 v_{s2}} \quad \text{Eq. 8}$$

These models are entirely dependent on metrics derived from the radiological signature of the annulus and the performance of the detector it is measured with. In using these approaches, estimates of the sample's m_{eff} can be made when its exact isotopic composition and mass is unknown. For these calculations, the specific spontaneous fission rate, F , is taken as 473 fissions per second per gram, and the (α, n) to spontaneous fission neutron ratio, α , is assumed to be zero, given that the materials being examined in this

study are highly-pure plutonium samples with small americium impurities. Additionally, the ε term refers to the detector's neutron detection efficiency at the location of the item during assay.

In addition to simply finding the values of $m_{eff,S}$, $m_{eff,D}$, and $m_{eff,M}$, we also evaluate the ratio of these values relative to the $m_{eff,K}$ of the sample, r_{e-k} . Finding these ratios serves two purposes; the estimated-known ratio can be used to benchmark the accuracy of the initial estimate, and the value of r_{e-k} can be leveraged to adjust the estimated m_{eff} by some correction factor such that its value more closely aligns with $m_{eff,K}$.

Upon executing the above-mentioned MCNP tests and assessing the equations for each annulus in our sample group, a dataset of actual and estimated values for M_L and m_{eff} is created for a multitude of possible annuli configurations. The actual values contained within this dataset will later serve as benchmarks by which the accuracy of the estimated leakage multiplier and effective mass values will be judged.

2.3. Correction Function Generation

As illustrated in Figures B.1, B.2, and B.3, point model-derived effective mass estimates for annuli are imperfect, and exhibit a pattern of overestimating m_{eff} at lower doubles rates, and underestimating m_{eff} at higher doubles rates. Additionally, the degree to which this behavior is pronounced is an artifact of the physical parameters of the annulus (Figure B.4). In all, to get better effective mass estimates, one must account for the effects the item's geometry have on its neutronics and radiological emissions, and correct for these behaviors.

To do so, this study employs correction functions and correction factors. Correction functions are functions which predict the value of a correction factor, c_f , which itself is some value that scales the value estimated for m_{eff} of an annulus such that it more closely aligns with $m_{eff,K}$ (i.e., r_{e-k} approaches unity). These functions are produced in five forms:

- 2nd order polynomial: $f_c = A \cdot x^2 + B \cdot x + C$
- Linear: $f_c = A + B \cdot x$
- Power-law: $f_c = A \cdot x^B$
- Exponential: $f_c = A \cdot e^{xB}$
- Logarithmic: $f_c = A + B \cdot \ln(x)$

Each correction function predicts the estimated-known m_{eff} ratio trend as a function of doubles rates. Additionally, the value of the correction functions' coefficients are determined by the values of the annuli's physical parameters.

2.4. Random Forest Models

To determine the value of coefficients governing these correction functions, random forest regression is performed. An initial set of 93 parameter-defined random forest models (RFMs) is formed. The size of this set reflects the number of unique combinations that can be formed from selecting one of the three estimator model, one of the five correction function forms, and a combination of any number of the annulus parameter (not parameter values) detailed in Table 1. For example, a single RFM will be produced to analyze SPM-based m_{eff} estimates that are corrected via a logarithmic function trained on annulus thickness, enrichment, and location data.

For each RFM, the 46,461 annuli in the training set are then organized into subsets, in which each annulus in the subset shares a common value for the annulus parameters the correction function is being trained on (Figure 2). Then, for each subset, the r_{e-k} value as determined by the chosen model (SPM, DPM, or MCM) of each annulus in the subset is plotted against its measured doubles rate, D , and a best-fit curve matching the function type specified by the correction function is calculated (Figure 3). The coefficients governing this curve, as well as the parameter values which define the subset, are recorded together. If such a curve cannot be created (say due to an insufficient number of data points being available for analysis), the process is stopped, the current RFM is removed from the set, and analysis on the next RFM begins.

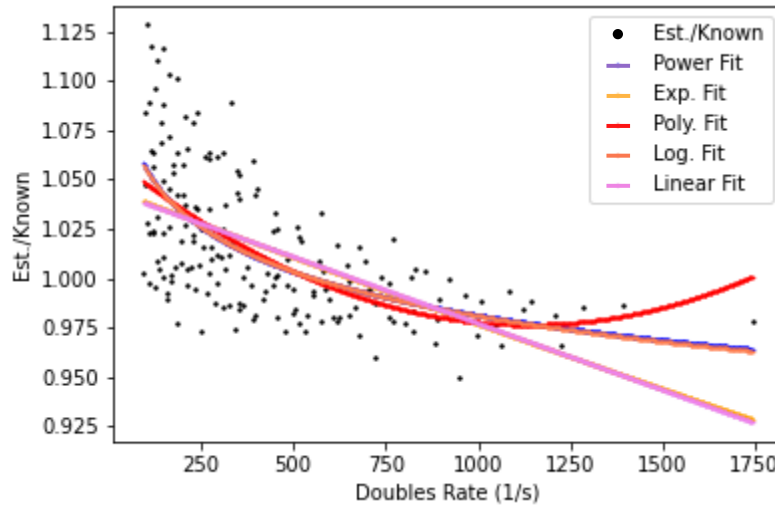
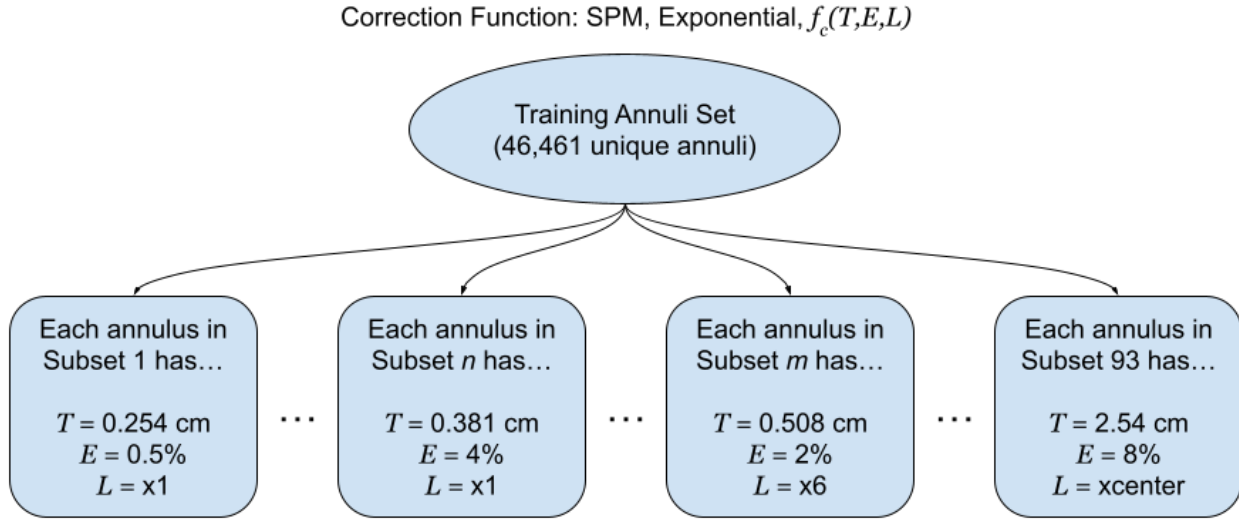


Figure 3: Correction function for thickness, enrichment, and location separated annuli using SPM estimates. All depicted annuli have the following properties: $t = 2.54$ cm, enrichment = 8%, located at x2.

Once every subset has been analyzed for a given correction function, a 100 decision tree random forest regression is performed to study how the best-fit coefficients change as the annulus parameters change. In all, this process yields 87 RFM which, theoretically, can be used to characterize the form of a correction function which produces a correction factor to improve the estimate of an annulus' effective mass.

After training the random forest models, a test set of 1,000 randomly generated annuli is produced such that the physical parameters present in this set are representative of those detailed in Table 1, but are not found in the training annulus set. For each annulus in this set, the random forest models are used to predict the correction factor for each individual annulus. This correction factor is then used to adjust the initial m_{eff} estimated value for the annulus (Eq. 9), producing a corrected effective mass estimate, $m_{eff,C}$. An additional corrected estimate-known effective mass value, $r_{e-k,C}$, is determined by simply taking the ratio of the corrected effective mass estimate and the known effective mass (Eq. 10). The collection of these values are then used to characterize the precision and accuracy of the individual random forest model's estimates, thus producing objective means by which the random forest models can be assessed.

$$m_{eff,C} = c_f \cdot m_{eff} \quad \text{Eq. 9}$$

$$r_{e-k,C} = \frac{m_{eff,C}}{m_{eff,K}} \quad \text{Eq. 10}$$

3. Results

3.1. Initial Estimator Performance

In comparing the initial, non-corrected estimated-known m_{eff} ratios produces by the SPM, DPM, and MCM models when applied to the test annuls datasets, the SPM method yields the most accurate initial effective mass estimates. On average, the estimated m_{eff} found using the SPM model is 4.1% greater than its $m_{eff,K}$ counterpart. Similarly, both the DPM and MCM also tend to overestimate an annulus' effective mass, with average estimated-known ratios of 6.3% and 6.7% above unity, respectively.

Estimator	\bar{x}	Min.	Max.	σ
SPM	1.041	0.950	1.132	0.0234
DPM	1.063	0.904	1.580	0.0443
MCM	1.067	0.797	1.654	0.0529

Table 2: r_{e-k} statistics for effective mass estimator models.

As illustrated in Figure 4, the MCM model-derived dataset, in addition to demonstrating the strongest bias, exhibits the largest standard deviation of m_{eff} estimates. The DPM and SPM methods produce improved results, with standard deviation values 16% and 56% smaller than that calculated for the MCM model, respectively. In their most extreme cases, the SPM, DPM, and MCM models yield m_{eff} estimates 13%, 58%, and 65% larger than the true effective mass of an annulus. This inaccuracy also manifests itself via underestimated m_{eff} values – SPM, DPM, and MCM models can underestimate the effective mass by as much as 5%, 10%, and 20%, respectively.

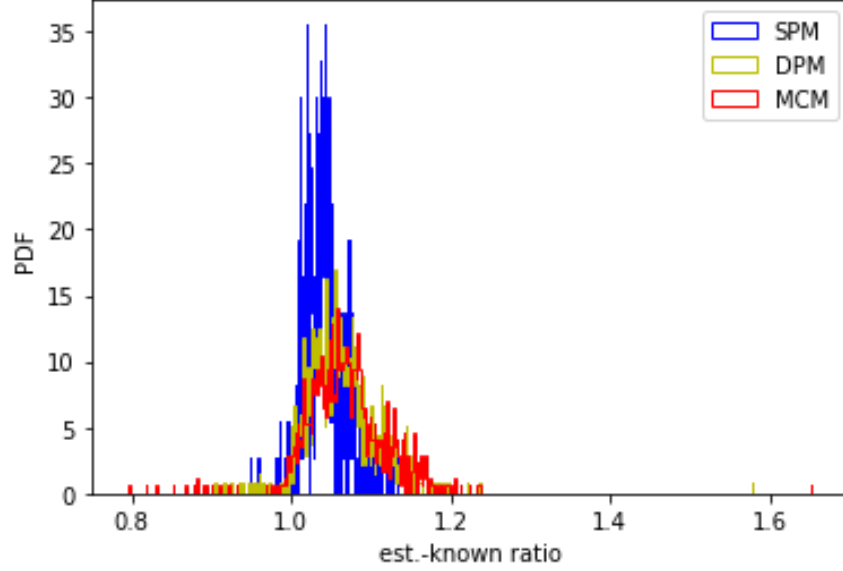


Figure 4: Histogram (500 bins) of r_{e-k} for all annuli using SPM, DPM, and MCM models. Plots are normalized such that the area under each curve is equal to one.

3.2. Random Forest Model and Correction Function Performance

Considering that the SPM, DPM, and MCM estimators are already capable of producing relatively accurate estimates of m_{eff} for a wide array of annuli. The need for correction functions arises from a need to reduce the variance within m_{eff} estimates due to the unaccounted for effects of the annulus' changing physical factors. However, the choice of which factors to isolate and which to ignore is not arbitrary. Correction functions which focus on too broad of an annulus subset (i.e., when only differentiating annuli by one physical parameter) have difficulty discerning meaningful trends within the m_{eff} - D relationship, and therefore only modestly improve accuracy and precision. However, a similar problem is encountered when too small of a subset of annuli is examined; when deriving correction functions relative to four or five physical parameters, meaningful trends between said parameters and r_{e-k} cannot be established, and the resulting correction functions.

The results of each RFM predictions as applied to the test annuli dataset were aggregated and analyzed to generate the average, minimum, and maximum corrected estimate-known effective mass ratio, $r_{e-k,C}$, values produced by the model. Standard deviations values for the sets of $r_{e-k,C}$ values were also calculated. For these identified metrics, all 87 random forest models were ranked by how well they performed under the following criteria; average $r_{e-k,C}$ values closest to 1, lowest maximum values of $r_{e-k,C}$, and which distribution of $r_{e-k,C}$ values yielded the smallest standard deviation. The models which best satisfied these criteria are identified in Table 3.

Metric of Best Performance	Correction Function	\bar{x}	Min	Max	σ
Average r_{e-k} value	Polynomial, MCM, $f_c(H, R, E, L)$	1.001	0.936	2.046	0.0478
Maximum r_{e-k} value	Polynomial, MCM, $f_c(T, E)$	1.032	1.004	5.679	0.1757
Smallest σ	Exponential, MCM, $f_c(T, R)$	1.005	0.883	1.007	0.0065

Table 3: Corrected r_{e-k} statistics for effective mass estimator models. Correction function variables refer to the variables outlined in Table 1 – annulus height, H , thickness, T , outer radius, R , nominal enrichment, E , and location within the detector, L .

The above-listed criteria represent how different models can be used to pursue different material accountancy goals. For example, if one prioritizes effective mass estimation accuracy over uncertainty, then a polynomial correction function, trained on annulus height, outer radius, enrichment, and location data, and used to augment MCM-derived m_{eff} values would be the preferred correction function model – this model, on average, yields the most accurate m_{eff} estimates. If, by contrast, an extremely conservative m_{eff} estimate is desired (say, a scenario in which underestimating the effective ^{240}Pu content of an annulus is unacceptable), the use of a polynomial correction function, trained on annulus thickness and enrichment data, should be used to refine initial MCM-derived estimates. The third criteria, the smallest standard deviation, is most useful when precise estimates of an annulus’ effective mass is of utmost importance, and uncertainty in said measurement must be minimized.

In all, the identified correction functions, and their RFMs, demonstrate the ability to more accurately estimate m_{eff} when appended to initial MCM estimates than any of the original point or multiplicity counting models can achieve (Figure 5). Additionally, of the three correction functions, both the four-factor MCM polynomial and two-factor MCM exponential functions produce estimates with vastly improved precision. As detailed in Table 4, $m_{eff,c}$ estimates vary from $m_{eff,k}$ by only -1.9/+2.4 % and -3.1/+0.7 % in 99% of all cases.

Correction Function	$P(r_{e-k} > x) = 0.995$	$P(r_{e-k} < x) = 0.995$	δx
Polynomial, MCM, $f_c(H, R, E, L)$	0.981	1.024	0.043
Polynomial, MCM, $f_c(T, E)$	1.004	2.117	1.113
Exponential, MCM, $f_c(T, R)$	0.969	1.007	0.038

Table 4: Confidence interval values for correction function performance.

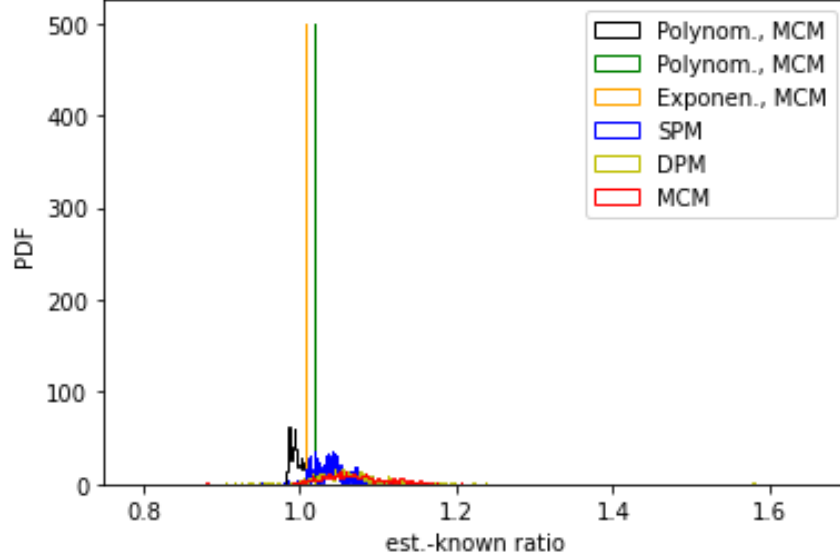


Figure 5: Histogram (500 bins) of all r_{e-k} values from both corrected and uncorrected datasets. Plots are overlaid to highlight the increased precision of the corrected estimates. A more detailed plot of the isolated correction function curves can be found in Figure B.5.

4. Conclusions

Estimating the effective mass of ^{240}Pu in Pu metal samples via existing point model and multiplicity counting models is a broadly generally accurate, yet imperfect practice. Factors, such as the physical form and enrichment of the sample, are not directly accounted for in these calculations, therefore allowing imprecision to manifest itself in the estimate. On average, this leads to the m_{eff} being approximately 1% higher than the actual effective mass of the sample. However, for sufficiently large or low activity samples, m_{eff} estimates may underestimate the actual effective mass by as much as 46% or overestimate by 18%.

In this study, we demonstrate a technique for mitigating this issue in which existing m_{eff} estimation processes are adapted to include correction factors. In training a random forest model to predict the degree to which existing effective mass calculations strays from truth using the physical parameters of the sample being assayed as input, the imprecision and inaccuracy of the initial effective mass estimate can be corrected, producing m_{eff} estimates for samples which more closely align with their true values. As revealed by the results outlined in this paper, a MCM-produced m_{eff} estimate adjusted by a correction factor calculated with an exponential correction function trained on annulus thickness and outer radius data performs this task the most successfully. Using this approach on the test set explored in this study, the average r_{e-k} value remained within 1% of unity, and the standard deviation of estimated effective masses relative to the known effective mass was reduced to 0.0065, constituting a 72%-98% improvement relative to the un-corrected singles point, doubles point, and multiplicity counting models. While this performance is comparable to the four-factor MCM polynomial correction function, the better precision coupled with the reduced tendency to overestimate the annulus' m_{eff} by such relatively large factors make the two-factor exponential MCM correction function the preferred choice.

Acknowledgements

The authors of this work would like to thank Los Alamos National Laboratory for sponsoring this research.

Funding

This work has been authored by an employee of Triad National Security, LLC, operator of the Los Alamos National Laboratory under Contract No.89233218CNA000001 with the U.S. Department of Energy.

References

- [1] D. K. Hauck, V. Henzl. "Spatial Multiplication Model as an Alternative to the Point Model in Neutron Multiplicity Counting." Los Alamos National Laboratory report, LA-UR-14-21991. (2014).
- [2] M. S. Krick, W. H. Geist, D. R. Mayo. "A Weighted Point Model for the Thermal Neutron Multiplicity Assay of High-Mass Plutonium Samples." Los Alamos National Laboratory report, LA-14157. (2005).
- [3] C. J. Thompson, B. E. O'Neil, W. S. Charlton. "A Random Forest Approach for Estimating Leakage Multiplication of Cylinders." Proceedings of the INMM 61st Annual Meeting. (2020).
- [4] C. J. Werner. "MCNP User's Manual – Code Version 6.2." Los Alamos National Laboratory report, LA-UR-17-29981. (2017).
- [5] N. Ensslin, W. C. Harker, M. S. Krick, D. G. Langner, M. M. Pickrell, J. E. Stewart. "Application Guide to Neutron Multiplicity Counting." Los Alamos National Laboratory report, LA-13422-M. (1998).
- [6] S. Tobin, M. Swinhoe, D. Beddingfield, J. Hendricks. "MCNPX & Multiplicity." Los Alamos National Laboratory report, LA-CP-06-1337. (2006).
- [7] D. Reilly, N. Ensslin, H. Smith, Jr., S. Kreiner. "Passive Nondestructive Assay of Nuclear Materials." Los Alamos National Laboratory report, LA-UR-90-732. (1991).

Appendix A:

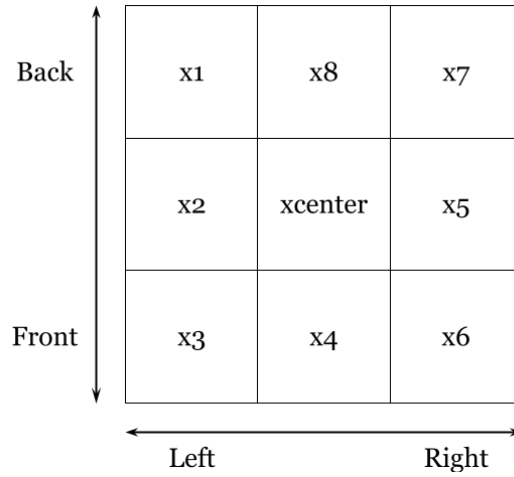


Figure A.1: Annulus locations within blister box. View from above.

Radius Number	Outer Radius (cm)				
	$t = 0.254$ cm	$t = 0.381$ cm	$t = 0.508$ cm	$t = 1.270$ cm	$t = 2.540$ cm
r1	0.49530	0.61595	0.73660	1.46050	2.66700
r2	0.73660	0.85090	0.96520	1.65100	2.79400
r3	0.97790	1.08585	1.19380	1.84150	2.92100
r4	1.21920	1.32080	1.42240	2.03200	3.04800
r5	1.46050	1.55575	1.65100	2.22250	3.17500
r6	1.70180	1.79070	1.87960	2.41300	3.30200
r7	1.94310	2.02565	2.10820	2.60350	3.42900
r8	2.18440	2.26060	2.33680	2.79400	3.55600
r9	2.42570	2.49555	2.56540	2.98450	3.68300
r10	2.66700	2.73050	2.79400	3.17500	3.81000
r11	2.90830	2.96545	3.02260	3.36550	3.93700
r12	3.14960	3.20040	3.25120	3.55600	4.06400
r13	3.39090	3.43535	3.47980	3.74650	4.19100
r14	3.63220	3.67030	3.70840	3.93700	4.31800
r15	3.87350	3.90525	3.93700	4.12750	4.44500
r16	4.11480	4.14020	4.16560	4.31800	4.57200
r17	4.35610	4.37515	4.39420	4.50850	4.69900
r18	4.59740	4.61010	4.62280	4.69900	4.82600
r19	4.83870	4.84505	4.85140	4.88950	4.95300
r20	5.08000	5.08000	5.08000	5.08000	5.08000

Table A.1: Outer radius number key and values by annulus ring thickness.

Appendix B: Supplemental Plots

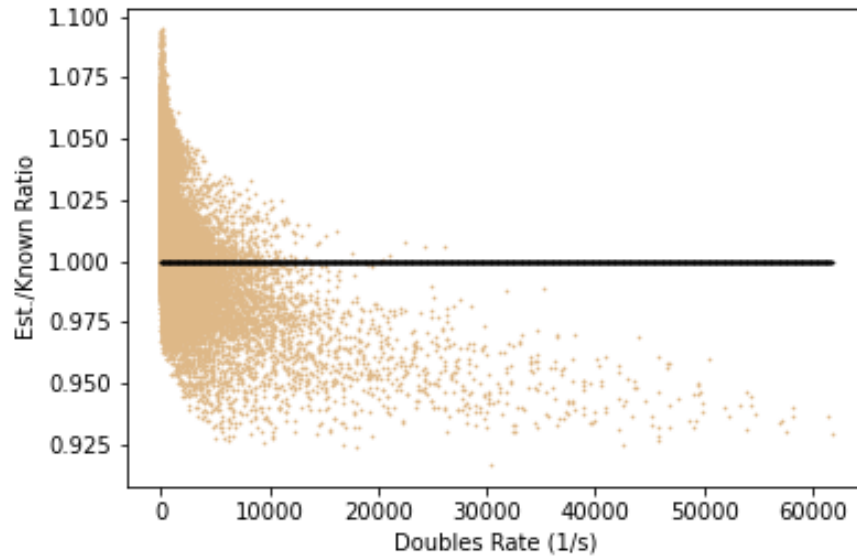


Figure B.1: Uncorrected SPM r_{e-k} values. The black line symbolized perfect m_{eff} estimate relative to the known value.

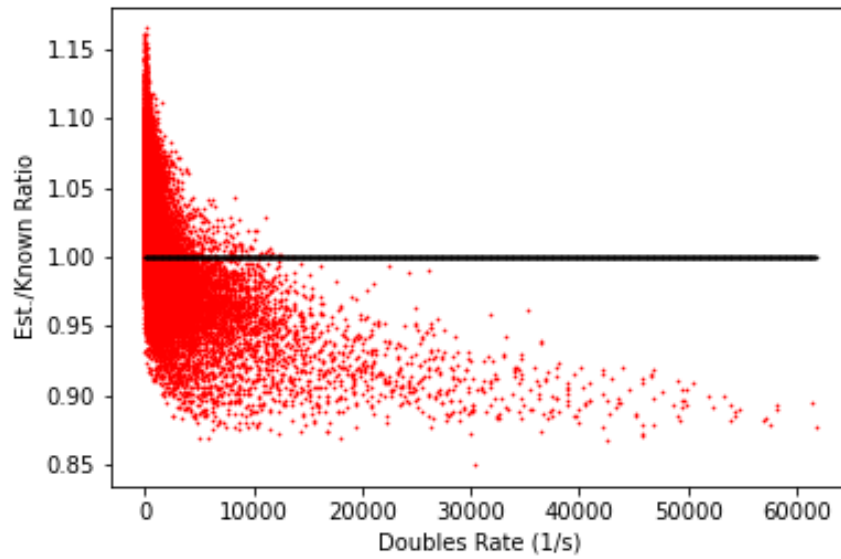


Figure B.2: Uncorrected DPM r_{e-k} values. The black line symbolized perfect m_{eff} estimate relative to the known value.

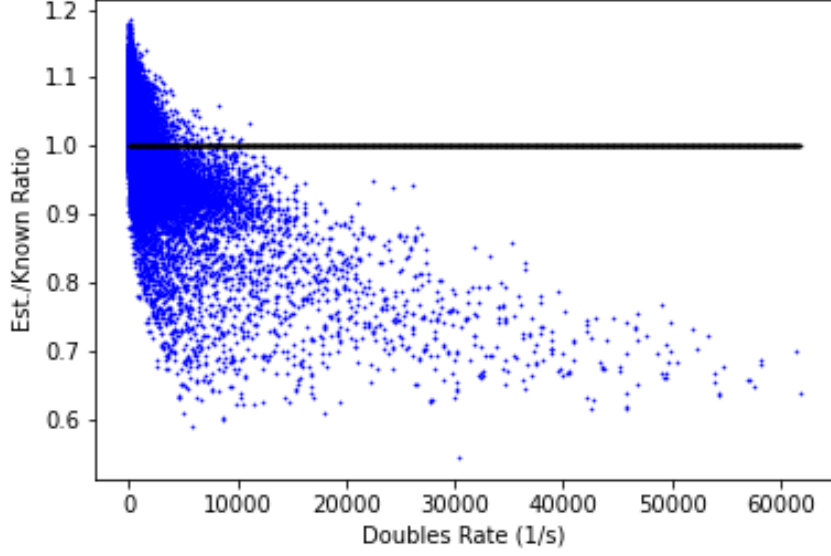


Figure B.3: Uncorrected MCM r_{e-k} values. The black line symbolized perfect m_{eff} estimate relative to the known value.

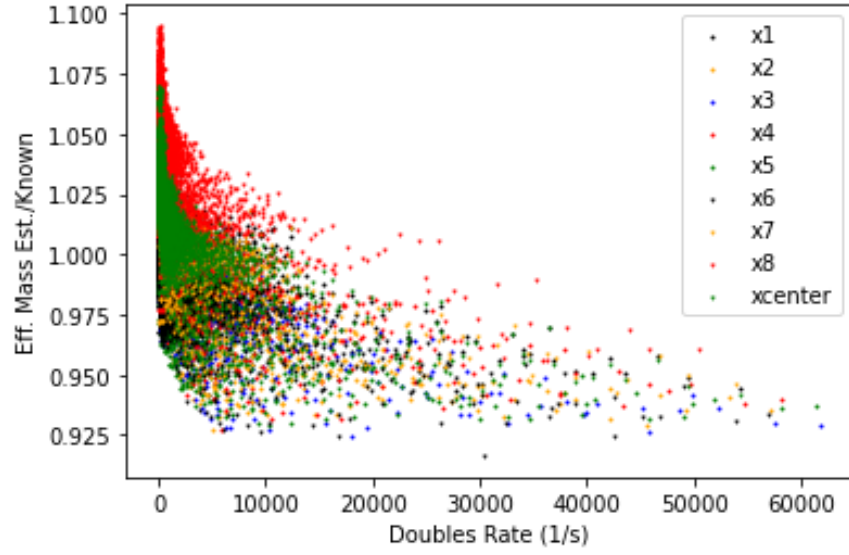


Figure B.4: Uncorrected SPM r_{e-k} values as a function of the detected doubles rate, D , for all training annuli. As the sections of solid reveal, m_{eff} estimates are noticeably biased, either high or low, based on where within the detector the annulus is placed (i.e., its “x location”).

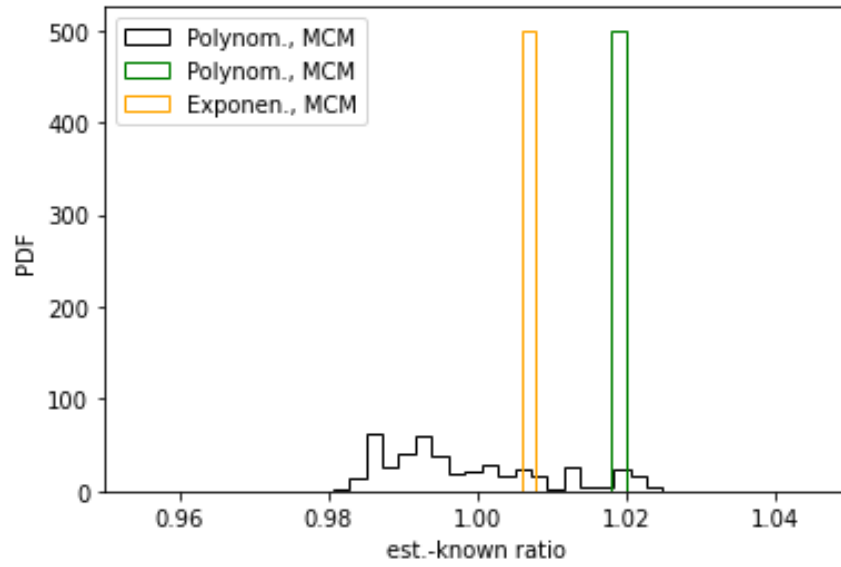


Figure B.5: Histogram (500 bins) of corrected r_{e-k} values from highlighted correction functions as described in Table 3. Plots are normalized such that the area under each curve is equal to one.